The Astrophysical Journal Letters, 897:L10 (8pp), 2020 July 1 https://doi.org/10.3847/2041-8213/ab6a18

The Extreme Space Weather Event in 1903 October/November: An Outburst from the Quiet Sun

Hisashi Hayakawa[1,2,3,4], Paulo Ribeiro[5,6], José M. Vaquero[7], María Cruz Gallego[7,8], Delores J. Knipp[9,10], Florian Mekhaldi[11], Ankush Bhaskar[12,13], Denny M. Oliveira[13,14], Yuta Notsu[15,16], Víctor M. S. Carrasco[7,8], Ana Caccavari[17], Bhaskara Veenadhari[18], Shyamoli Mukherjee[18], and Yusuke Ebihara[19]
[1] Graduate School of Letters, Osaka University, Toyonaka, Japan; hayakawa@kwasan.kyoto-u.ac.jp, hisashi@nagoya-u.jp
[2] Rutherford Appleton Laboratory, Chilton, UK
[3] Institute for Space-Earth Environmental Research, Nagoya University, Nagoya, 4648601, Japan
[4] Institute for Advanced Researches, Nagoya University, Nagoya, 4648601, Japan
[5] CITEUC, Centre for Earth and Space Research of the University of Coimbra, Portugal; pribeiro@ci.uc.pt
[6] Geophysical and Astronomical Observatory of the University of Coimbra, Portugal
[7] Instituto Universitario de Investigación del Agua, Cambio Climático y Sostenibilidad (IACYS), Universidad de Extremadura, Badajoz, Spain
[8] Departamento de Física, Universidad de Extremadura, Badajoz, Spain
[9] High Altitude Observatory, National Center for Atmospheric Research, Boulder, USA
[10] Smead Aerospace Engineering Sciences Department, University of Colorado Boulder, Boulder, USA
[11] Department of Geology-Quaternary Sciences, Lund University, Lund, Sweden
[12] Catholic University of America, Washington DC, USA
[13] NASA Goddard Space Flight Center, Greenbelt, MD, USA
[14] Goddard Planetary Heliophysics Institute, University of Maryland, Baltimore County, Baltimore, MD, USA
[15] Laboratory for Atmospheric and Space Physics, University of Colorado Boulder, Boulder, USA
[16] National Solar Observatory, Boulder, CO, USA
[17] Instituto de Geofísica, Unidad Michoacan, Universidad Nacional Autonoma de Mexico, Morelia, Mexico
[18] Indian Institute of Geomagnetism, Plot 5, Sector 18, New Panvel (West), Navi Mumbai, India
[19] Research Institute for Sustainable Humanosphere, Kyoto University, Uji, Japan
Received 2019 September 16; revised 2019 December 28; accepted 2019 December 28; published 2020 June 30

Abstract

While the Sun is generally more eruptive during its maximum and declining phases, observational evidence shows certain cases of powerful solar eruptions during the quiet phase of solar activity. Occurring in the weak Solar Cycle 14 just after its minimum, the extreme space weather event in 1903 October–November is one of these cases. Here, we reconstruct the time series of geomagnetic activity based on contemporary observational records. With the mid-latitude magnetograms, the 1903 magnetic storm is thought to be caused by a fast coronal mass ejection ($\approx$1500 km s^{-1}) and is regarded as a superstorm with an estimated minimum of the equivalent disturbance storm time index (Dst') of ≈ -531 nT. The reconstructed time series has been compared with the equatorward extension of auroral oval ($\approx 44\overset{\circ}{.}1$ in invariant latitude) and the time series of telegraphic disturbances. This case study shows that potential threats posed by extreme space weather events exist even during weak solar cycles or near their minima.

Unified Astronomy Thesaurus concepts: Solar-terrestrial interactions (1473); Solar coronal mass ejections (310); Solar flares (1496); Sunspots (1653); Geomagnetic fields (646); Solar storm (1526)

Supporting material: data behind figure

1. Introduction

The Sun occasionally causes magnetic storms as a consequence of interplanetary coronal mass ejections (ICMEs) with southward interplanetary magnetic field (IMF; e.g., Gonzalez et al. 1994; Daglis et al. 1999). Due to the growing dependence on technology-based infrastructure, our civilization is increasingly vulnerable to such space weather events. Recent analyses have estimated the possible effects of extreme magnetic storms to be potentially catastrophic to modern civilization, especially when they are as extreme as those in 1859 September and 1921 May (e.g., Baker et al. 2008; Riley et al. 2018).

Statistical studies have revealed that such extreme space weather events tend to occur around the maximum and in the declining phase of solar cycles (e.g., Lefévre et al. 2016; Meng et al. 2019). Indeed, the most extreme space weather events in observational history, such as those in 1859, 1872, 1909, 1921, and 1989 (e.g., Allen et al. 1989; Cliver & Dietrich 2013; WDC for Geomagnetism, Kyoto et al. 2015; Hayakawa et al. 2018, 2019a; Love et al. 2019a, 2019b), as well as the recent Halloween sequence in 2003 (e.g., Gopalswamy et al. 2005), have appeared in these phases of their corresponding solar cycles and make us wary of the Sun around the maximum to the declining phase.

However, observations show that even the quieter Sun can cause significant space weather events (e.g., Kilpua et al. 2015). The extreme storm in 1986 February occurred around the solar minimum with an intensity of standard disturbance storm time (Dst) = −307 nT (e.g., Garcia & Dryer 1987). The extreme storm of 1967 May (Dst = −387 nT) in the ascending phase of solar cycle 20 produced significant societal impacts (Knipp et al. 2016).

Exactly a century before the Halloween sequence in 2003, another "Halloween event" caused a significant magnetic disturbance and produced geomagnetically-induced currents (GICs; potentially harmful to modern power equipment and transmission lines) at mid-latitudes, resulting in the earliest documented communication-network disturbance in the Iberian Peninsula (Ribeiro et al. 2016). Interestingly, this storm occurred just after the minimum of a weak Solar Cycle 14.

Indeed, despite its lowest amplitude since the Dalton Minimum (see Clette & Lefévre 2016), Solar Cycle 14 hosted two major space weather events in 1903 (Ribeiro et al. 2016) and 1909 (Hayakawa et al. 2019a; Love et al. 2019a).

Here we analyze the space weather events in 1903 October/November from the solar photosphere to the ground terrestrial magnetic field. We first review the solar observational data around 1903 October/November and its flare onset on the basis of contemporary solar photospheric observations and magnetic measurements. We estimate the parameters of the source ICME on the basis of the propagation time and amplitude of the storm sudden commencement (SSC). We then locate and analyze four mid-latitude magnetograms and reconstruct an equivalent disturbance storm time index (Dst'), which allows assessment of the storm intensity. We document these results with the contemporary auroral visibility and GICs (see the Appendix), to provide a comprehensive overview of this space weather event during the early ascending phase of a weak solar cycle.

2. The Solar Surface in 1903 October/November

The Sun in the early 1900s was relatively quiet. With its onset in 1902 January, Solar Cycle 14 reached its maximal sunspot number ≈180 in 1907 February (Figure 1, top panel). This cycle amplitude was the lowest since the Dalton Minimum. On the surface of this quiet Sun, the sunspot group 5098 (Figure 1, bottom panel) appeared on the eastern limb of the southern hemisphere on 1903 October 25. It consisted of a relatively large composite group (493 millionths of solar hemisphere (msh); Jones 1955), which gradually broke up in its passage across the disk, becoming a long, irregular patch that reached the central meridian on October 31. This group disappeared from the western limb on November 6 (Royal Observatory 1905).

Favorably situated near the disk center, this sunspot was considerably active on 1903 October 29–31 (Fowler 1903; Jones 1955). Fowler (1903) reported "a violent distortion and reversal of the C line of hydrogen" near this group between 10–11 GMT on October 31. Similar reversals of the C line were seen on October 29 and 30, occasionally with more brightness but only with less distortion of the dark line, namely absorption lines (Fowler 1903, p. 6). The reversals of C line probably mean strong emission in Hα line during these flares and dynamic motion of plasma in the chromosphere (see, e.g., Ichimoto & Kurokawa 1984).

The occurrence of intense flares during this period is confirmed with a magnetic crochet, i.e., solar flare effect (see Jones 1955). Figure 2 shows a magnetic crochet of ≈15 nT at ≈02 GMT (13.5 local time = LT) on October 30 recorded by the Christchurch magnetogram (S43°32′, E172°37′) in New Zealand (Marchant 1904; 144/145). The solar flare was followed by a high-velocity coronal mass ejection (CME) directed toward the Earth. Based on the Coimbra magnetogram in Portugal, the interplanetary CME (ICME) driving shock caused a sharp SSC at ≈5.5 GMT on October 31 with an amplitude of at least 70 nT (Ribeiro et al. 2016). However, according to the ≈12 LT Colaba magnetogram in British India (based on the vectorial digitizing of the analog curves), the SSC occurred at 05.35 GMT (10.85 LT) with amplitude of ≈98 nT (and an average increasing rate of 4.6 nT min^{-1}). This lets us compute the ICME propagation time as ≈27.5 hr, slightly shorter than 28 h estimated from Zo-sé magnetogram in China (Jones 1955), and estimate the average ICME speed as ≈1500 km s^{-1}. Substituting the Colaba's SSC amplitude (≈98 nT) into empirical equations in Araki (2014), we estimate a solar wind dynamic pressure jump of ≈42.7 nPa. Assuming that the solar wind consists mostly of protons, the downstream solar wind density is estimated to be ≈11.4 cm^{-3}.

Interestingly, the magnetograms at Colaba (Figure 3) and Coimbra (Figure 4 of Ribeiro et al. 2016) show sudden impulses after 20.5 GMT on 1903 October 31. These impulses suggest that this storm was probably even more complex in its structure. They presumably are due to a sudden change in solar wind dynamic pressure indicating compression of the magnetosphere, shock/sheath, or ICME before the main ICME, as are the cases with the extreme storms in 1967 and 1989 (Knipp et al. 2016; Boteler 2019).

3. Magnetic Observations in 1903

After the SSC and variations of the initial phase, great magnetic disturbances were reported globally. However, many of the stations saw their recordings interrupted or incomplete due to off-scale problems associated with the fast and extreme amplitude of magnetic oscillations. The Dst is a global index used to measure the geomagnetic activity and assess the intensity of magnetic storms. The index is derived from magnetograms of horizontal force (H) recorded at four middle- to low-latitude standard stations (Kakioka, Japan; Hermanus, South Africa; San Juan, Puerto Rico; Honolulu, Hawaii; Sugiura 1964). With the aim of assessing the severity of the 1903 storm, we first attempted to obtain the magnetograms of the historical stations closest to the ones used in the calculation of standard Dst'. Unfortunately, nearby surrogates for each standard station were either off scale or not in operation.

We therefore surveyed magnetic observations in four mid- to low-latitude stations with a fairly even longitudinal distribution around the Earth. We found a rather complete set of recordings and hourly data for the following observatories, for which we computed their magnetic latitude (MLAT) and longitude (MLON) in 1903 with IGRF12 model (Thébault et al. 2015), as summarized in Table 1.

To obtain the hourly averages from the analog magnetograms, we traced the curves with vector-graphic programs and converted their amplitude from mm to nT. For COI, after the vectorization and digital reconstruction, we printed the magnetic curves (keeping the scale values) and measured the hourly mean values of H by hand (following the procedure that was commonly used for reading the classic analog magnetograms). For CLA and CUA the hourly means were obtained by simply averaging the digitized value (CLA and CUA) values obtained during the digitization procedure, in comparison with recorded scales. The CLA digitization has been compared with Moos' trace for calibration. For ZKW, we only have the published tables presumably with the hourly spot values, and therefore we used these as an equivalence of hourly averages. To obtain more consistent time series with ZKW, hourly data from COI, CLA, and CUA observatories were calculated as hour-centered averages (i.e., 00:00, 01:00, 02:00, etc.), allowing a properly averaging in the Dst' estimate.

Note that CLA's original magnetogram shows a broken behavior, with simultaneous instrumental jumps of the H curve and its baseline (Figure 3). To reconstruct the natural trace of H we assumed the continuity of the respective baseline. In the present reconstruction of time series of CLA, we need to carefully compare the original magnetograms and the reconstruction in Moos (1910), which shows a gap in the H

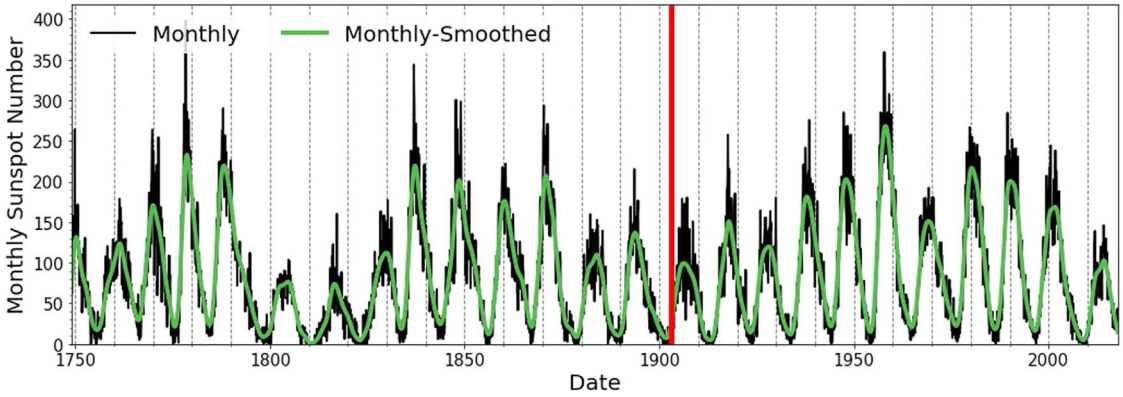

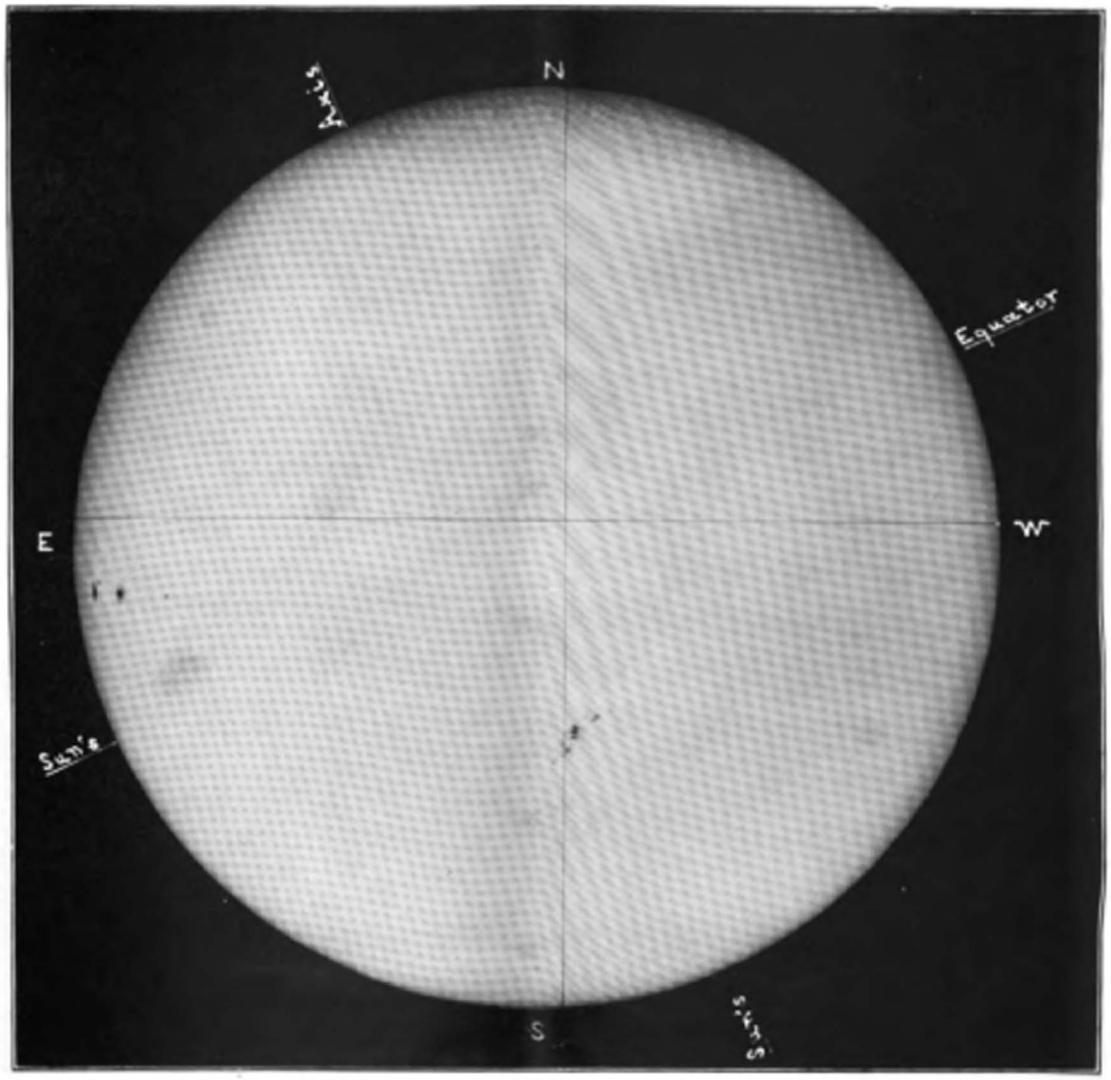

PHOTOGRAPH OF THE SUN.

1903. October 31d. 10h. 24m. 28s., Greenwich Civil Time.

Taken at the Royal Observatory, Greenwich, with the Dallmeyer Photoheliograph. Aperture 4 inches; reduced to 2·9 inches.

Figure 1. Top panel: monthly (black color) and monthly smoothed (green color) sunspot number (version 2; see Clette & Lefévre 2016). The vertical red line indicates the year 1903, when this study case occurred. Bottom panel: photograph of the Sun at 10.4 UT on 1903 October 31, taken at the Royal Observatory, Greenwich, UK, derived from Maunder (1903).

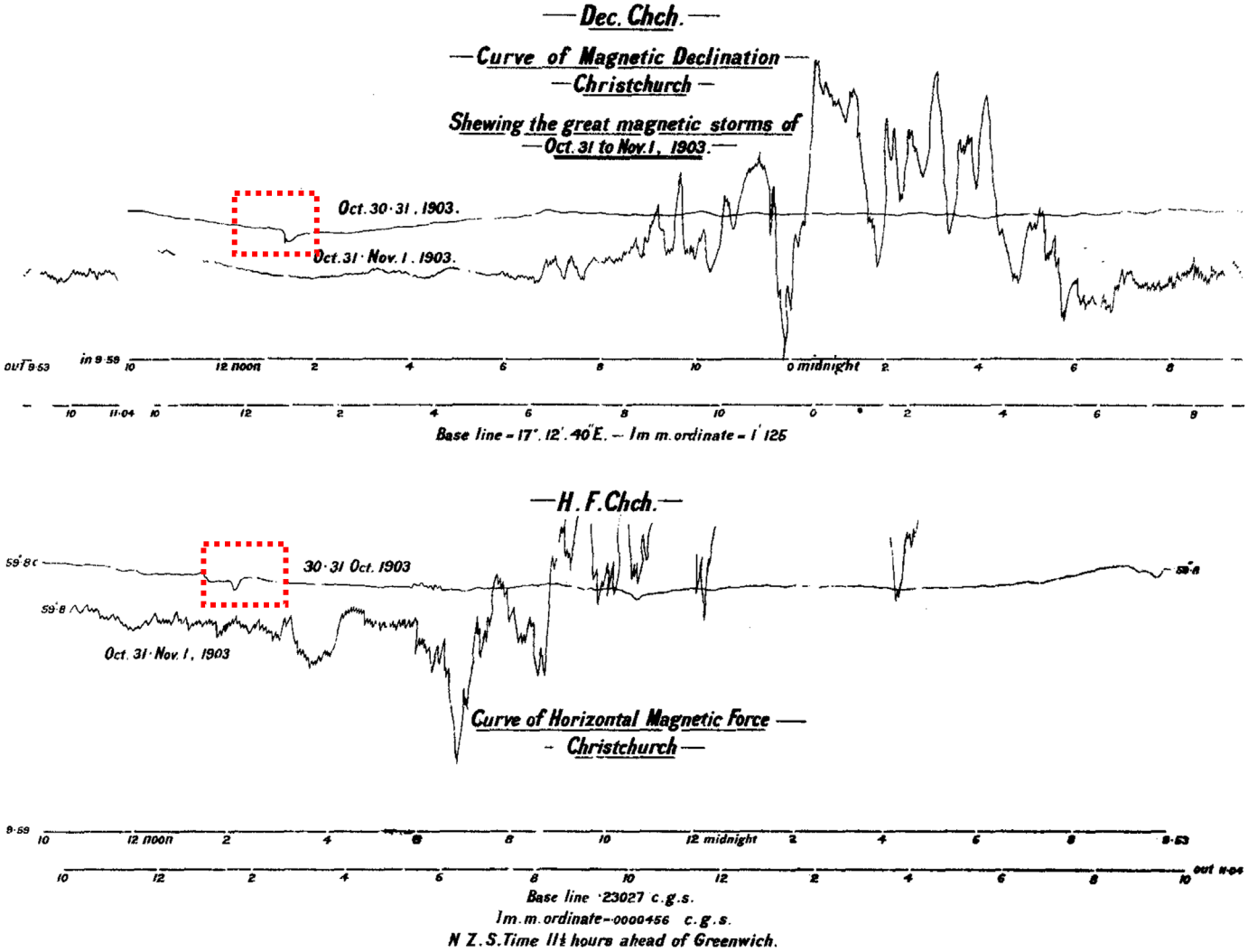

Figure 2. Magnetic crochets (enclosed by red squares) recorded in the Christchurch magnetogram (Marchant 1904, 144/145), showing the horizontal force in the upper panel and the decl. in the lower panel. The negative direction of the horizontal force is shown upward in this magnetogram.

recording. In this regard, we narrowly inspected the copies of the original curves (Figure 3), and we estimated the duration of the referred gap, on the basis of the length of each baseline bar (corresponds to 2 hr of recording) and the inserted handwritten notes on the start and end times of the record. Our measurement shows that the H recording in the upper panel of Figure 3 ends at ∼13.7 LT and restarts in the lower panel at ∼15.2 LT, resulting in a data gap of ∼1.5 hr between 8.7 GMT and 10.2 GMT.

4. Time Series and Intensity of the 1903 October/November Storm

The obtained hourly averages of H for each analog magnetograms in COI, CLA, and CUA were compared with the corresponding tabulated hourly values found for the ZKW observatory. As shown in Sugiura (1964), the disturbance at each observatory is defined as

$$D_o(t) = H_o(t) - B_o - Sq_o(t).$$

Here, the subscript "o" refers to each observatory, and H_o, B_o, and Sq_o stand for observed H, baseline of H, and solar quiet daily variation as quasi-daily variation of H, respectively. We approximated B_o with the pre-storm level, H hourly value at 16.5 GMT of October 30, as corresponding to the calm period before the arrival of the storm in each station. We also approximated the Sq variation of each station with the average daily variation of 5 quiet days of 1903 October (21, 20, 9, 24, 16), which were selected based on the revised daily Aa index (Lockwood et al. 2018). We then weighted D_o (t) of each observatory with their MLATs (λ), and obtained their average as a Dst' estimate. Figure 4 shows the hourly D_o $(t)/\cos\lambda$ of the reference stations, COI, CLA, CUA, and ZKW, as well as the Dst' time series as their average.

After the SSC around 5.5 GMT on October 31, the Dst' time series shows a sharp decrease from ≈06 GMT, reaching its minimum −531 nT at 15 GMT. The storm main phase seems to have ended by ≈16 GMT, and a relatively long recovery phase followed it. Contemporary estimates based on off-scaled magnetograms of Tokyo, Cheltenham (Maryland, USA), and Baldwin (Kansas, USA) point to amplitudes with latitudinal weighting of 571 nT, 805 nT, and 1010 nT, respectively (Bauer 1904; Okada 1904). In addition to confirming our estimate, these additional data suggest that the storm may have been even more intense.

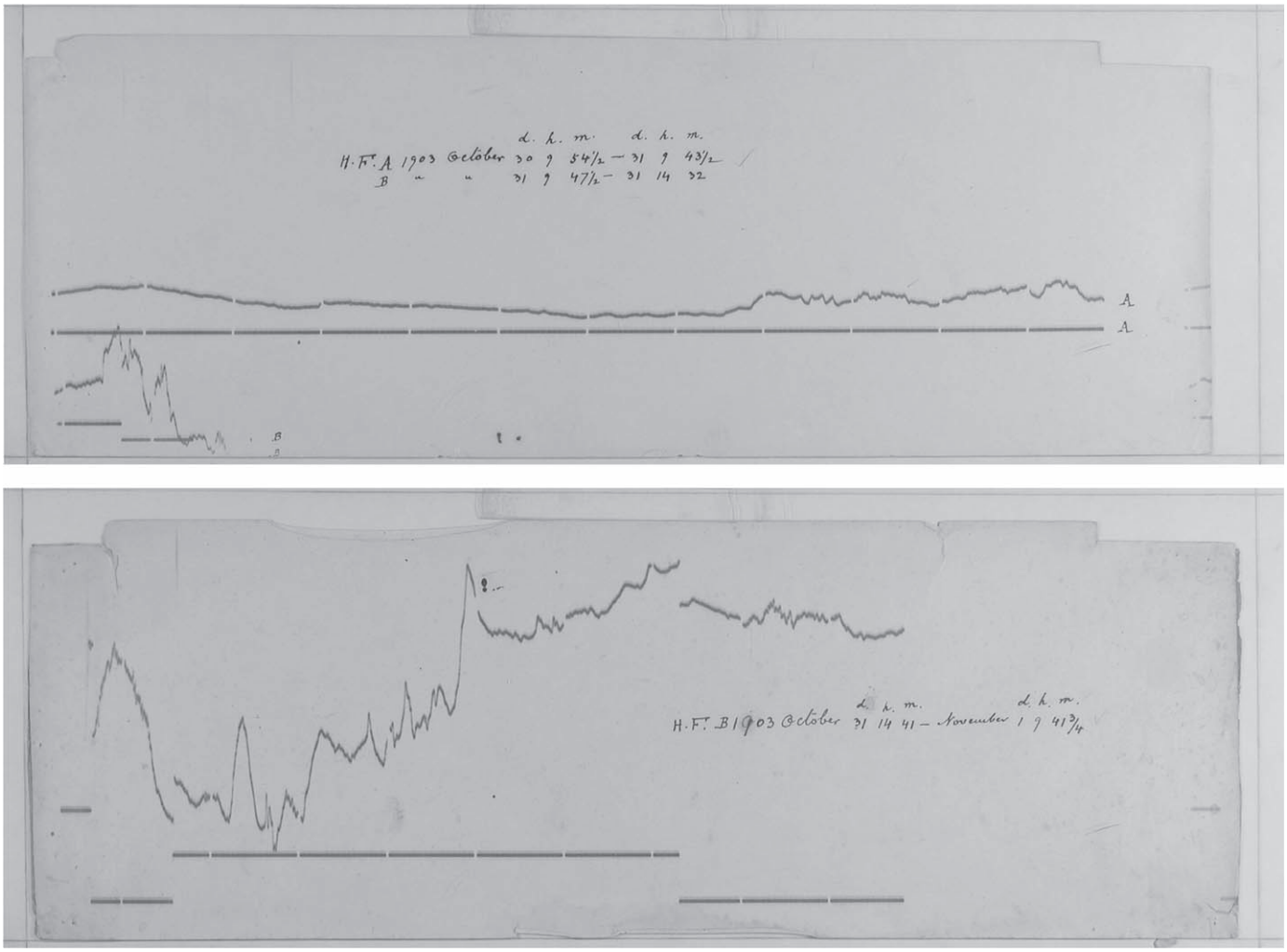

Figure 3. Original Colaba magnetogram on 1903 October 31–November 1, adopted from the WDC for Geomagnetism at Kyoto (http://wdc.kugi.kyoto-u.ac.jp/film/index/cla_1903_normal-j.html). Each bar of baseline shows a duration of 2 hr after the record start at 10 LT (Moos 1910, p. 251). We assumed the continuity of baseline to reconstruct the magnetogram. (Courtesy of WDC for Geomagnetism at Kyoto and Colaba Observatory (current under administration of the IIG)).

The minimum Dst' value of −531 nT obtained for the 1903 storm ranks between the largest (1989 March; −589 nT) and the second-largest (1959 July; −429 nT) magnetic storm of the official Dst index in the post-International Geophysical Year 1957–1958 interval. It should be highlighted that this extreme storm occurred at the onset of the weak Solar Cycle 14, while the other well-known five extreme storms (Dst'/Dst $\leqslant -500$ nT, 1859, 1872, 1909, 1921, and 1989) occurred around the maximum or in the declining phases of their corresponding solar cycle (Tsurutani et al. 2003; Cliver & Dietrich 2013; Hayakawa et al. 2018, 2019a, 2019b; Love et al. 2019a, 2019b).

5. Consequence of the Extreme Storms, Aurorae, and Space Weather Hazards

This magnetic storm caused great auroral displays and space weather hazards (see the Appendix). The aurorae were widely seen in the territories of the Russian Empire, Australia, New Zealand, and the United States (Figure 5). The auroral visibility was reported down to Irkoutsk (Russia; N40°.9 MLAT) and Walcha (Australia; S39°.4 MLAT) in northern and southern hemispheres (OPCN 1906; The Walcha Witness and Vernon County Record, 1903 November 7, p. 2). As the aurora was reported overhead at Sydney, Australia (−42°.2 MLAT; Lockyer 1903), the footprint of the magnetic field line for its equatorward boundary of the auroral oval is conservatively reconstructed as ≈44°.1 invariant latitude (ILAT), according to the procedure in Hayakawa et al. (2018). This is almost consistent with the auroral displays in the American sector, reported overhead at Leadville, CO (*Herald Democrat*, 1903 November 1, p. 2; 47°.9 MLAT) and covering all of the sky at Yerkes Observatory, WI (Barnard, 1910; 53°.1 MLAT). On the other hand, the aurorae were not significantly reported in the European sector, probably because the storm main phase occurred around 6–16 hr GMT, i.e., during daytime. The European observers saw aurorae probably around the late storm recovery phase.

As also shown in Ribeiro et al. (2016), the telegraph communication network was interrupted in the Iberian Peninsula during 9.5–21 GMT, with its maximum intensity occurring during 12.5–15 GMT. This maximum disturbance coincides exactly with the negative peak of the Dst' time series during 12–16 GMT, where the Dst' intensity surpassed <-400 nT (see Figure 4). Likewise, the communications from Paris to North America and Mediterranean countries had been reportedly interrupted from ≈9 GMT to sunset, although with a temporary recovery of normal operating conditions between ≈16.75–17.5 GMT (Lockyer 1903).

Table 1
Reference Stations used in this Article

Observatory	Geographic Lat.	Geographic Long.	MLAT	MLON	Time Difference	Max ΔH Range	Reference
Coimbra (COI)	N40°13′	W8°25′	N45.°0	E69.°9	≈GMT ± 0	707	R16
Colaba (CLA)	N18°54′	E72°49′	N9.°9	E143.°4	≈GMT+5	777	WDC-Kyoto
Cuajimalpa (CUA)	N20°53′	W100°53′	N30.°4	W35.°2	≈GMT–7	570	UNAM
Zi-Ka-Wei (ZKW)	N31°13′	E121°26′	N20.°0	E170.°7	≈GMT+8	636	Z06

Note. MLAT and MLON stand for magnetic latitude and magnetic longitude, respectively. The time difference is shown referencing the Greenwich Mean Time (GMT), as defined in each observatory. The maximum range is shown in spot value with latitudinal weighting. The reference column shows where these data and details are derived from Ribeiro et al. (2016; R16), Zi-Ka-Wei (1906, pp. 38–39; Z06), WDC for Geomagnetism at Kyoto, and Universidad Nacional Autónoma de México (UNAM). The value is converted from mm to nT, according to their scale values: 7.7 nT mm^{-1} (COI; Ribeiro et al. 2016), 17 nT mm^{-1} (CUA), and 5.12 and 4.72 nT mm^{-1} (CLA: October and November; Moos 1910).

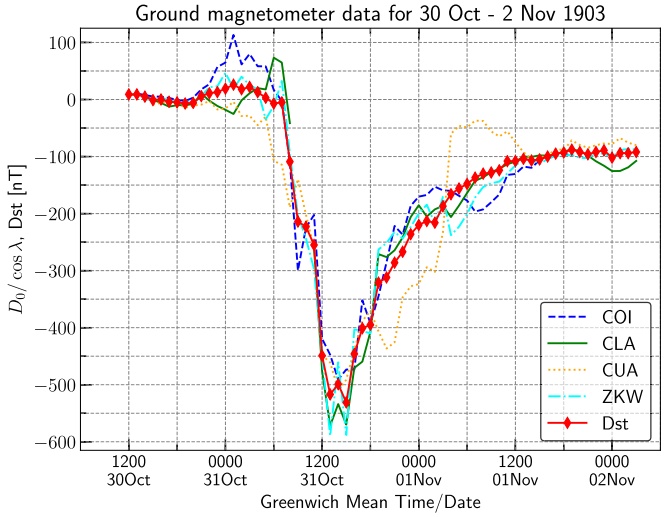

Figure 4. The plot shows D_0 on 1903 October 30–November 2 of the reference stations, COI, CLA, CUA, and ZKW, as well as reconstructed Dst' estimate. As the CLA magnetogram is scaled off at 9–10 h GMT, the Dst' estimate in this period is reconstructed with data from three stations. Their background data are provided as data behind the figure.

(The data used to create this figure are available.)

This interruption mostly coincides with the period with its Dst' value more negative than −200 nT.

The GICs hit London and disturbed its railway system and telegraph connections with Latin America, France, Italy, Spain, Portugal, and Algeria (Maunder 1903). Likewise, in the United States, this storm affected telephone lines around Chicago with extreme voltage of 675 volts of electricity in the wires and considered "enough to kill a man" (The Chicago Sunday Tribune, 1903 November 1, p. 8). In New South Wales of Australia, where aurora was reported overhead (Lockyer 1903), telegraph disturbances were reported at least between 6 and 10.25 GMT (Klotz 1904). Klotz (1904, p. 188) reported that "the telegraph lines running in a southerly direction were most violently affected."

6. Discussion and Concluding Remarks

In this Letter, we aimed to provide a comprehensive view of the extreme storm of 1903 October 31, by analyzing data of the causal chain between solar photosphere to the ground terrestrial magnetic field. The Sun was rather quiet in 1903, during the second year of the ascending phase of the weak Solar Cycle 14.

Nonetheless, a relatively large composite sunspot group (5098) appeared on the eastern limb of the southern hemisphere on 1903 October 25, evolving gradually in its passage across the disk until becoming a long and irregular patch upon arrival at the central meridian on October 31. The apparent complex morphological evolution of this active region was accompanied by a set of highly energetic flares between October 29 and 31 (Fowler 1903). In particular, the flare at ≈02 GMT on October 30 was intense enough to be recorded as a magnetic crochet in the Christchurch magnetogram (Figure 2).

The related ICME hit the magnetosphere ≈28 hr later, with the shock being recorded in the magnetograms of Coimbra and Colaba as a strong SSC around 5:30 GMT on October 31. According to our estimate, the ICME propagated into the interplanetary space with an average speed of ≈1500 km s^{-1}, and a solar wind pressure increment and density of ≈42.7 nPa, and ≈11.4 cm^{-3}, respectively.

In addition, the IMF was strongly southward as suggested by the great storm recorded by magnetograms of four observatories at mid-MLATs (Coimbra, Cuajimalpa, Colaba, and Zi-ka-wei). On this basis, an alternative Dst' time series has been reconstructed for the 1903 storm (Figure 4), showing that the storm's main phase lasted for almost 10 hr and reached a maximum negative value of ≈−531 nT, which ranks between the largest (1989 March; −589 nT) and the second-largest (1959 July; −429 nT) magnetic storms within the official Dst index.

This extreme storm caused significant auroral displays and space weather hazards. Aurorae were reported at least down to ∼40° MLAT in both hemispheres and the equatorward boundary of auroral oval has been conservatively reconstructed at 44.°1 ILAT. The telegraph and telephone lines in France, Iberian Peninsula, and even Algeria were significantly affected mostly during the storm main phase. At London, the railway system was also affected. At Chicago, an extreme voltage level of ≈675 volts associated with extreme GICs were reported as "enough to kill a man."

It is possible that this ICME was accompanied by solar energetic particles (SEPs). A preliminary survey of the Greenland ice core data from NGRIP and Dye-3 shows an enhancement in ^{36}Cl concentrations in the early 1900s. However, the ^{10}Be data show only a small peak using the residuals obtained by subtraction of the solar 11 yr cycle in the same ice cores (Beer et al. 1990; Berggren et al. 2009; McCracken & Beer 2015; Mekhaldi 2019). This may indicate that the SEP associated with the CME was not large enough to produce enough ^{10}Be as opposed to ^{36}Cl, or the ICME did not direct a SEP event at Earth (see e.g., Gopalswamy et al. 2012; Usoskin & Kovaltsov 2012). However, this needs to be treated with caution until additional ice core data can complement

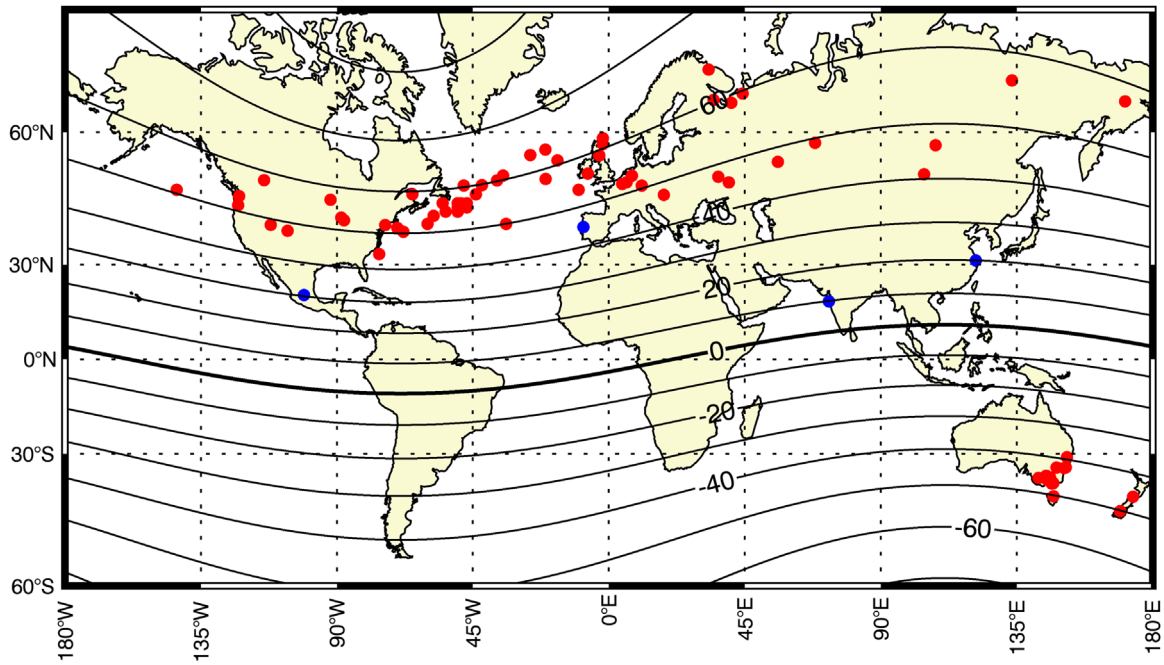

Figure 5. Auroral visibility between 1903 October 30 and November 1. The red dots show auroral observational sites in this interval of time (see the Appendix), whereas blue dots show the reference geomagnetic stations we used in this study (see Table 1). The magnetic latitude is computed on the basis of dipole assumption of IGRF12 model (Thébault et al. 2015).

these results and can rule out system effects that sometimes lead to coincidental peaks.

Although we are aware of the typical concentration of extreme space weather events around the maximum to the declining phase of solar cycles (e.g., Lefévre et al. 2016), the Sun is capable of launching highly geo-effective ICMEs, which in turn result in extreme space weather events even during its quiet phase, and even for a weak solar cycle, like Solar Cycle 14. Anyone who makes or uses space weather forecasts should be aware the potential of extreme space weather events even as the Sun transitions from solar minimum to the upcoming Solar Cycle 25.

We thank World Data Center for Geomagnetism, Kyoto, for providing the observational results from Tokyo, Vieques, and Honolulu, as well as the digital images of Colaba magnetograms and the scale unit of Colaba magnetograms, Tony Hurst and Tanja Petersen for scale unit of Christchurch magnetogram, Craig Rodger for his advice on the NZ geomagnetic measurements at that time, Sunspot Index and Long-term Solar Observations (SILSO) for providing the international sunspot number, the University of Coimbra for providing Coimbra magnetograms, and Universidad Nacional Autónoma de México (especially Juan Esteban Hernández Quintero, Gerardo Cifuentes-Nava, and Armando Carrillo-Vargas) for providing Cuajimalpa magnetograms. We thank Colaba Observatory (now administrated by Indian Institute of Geomagnetism, India), Cuajimalpa Observatory, and Zi-ka-wei Observatory, and Coimbra Observatory for the recording of magnetic field measurements. CITEUC is funded by National Funds through FCT-Foundation for Science and Technology (project: UID/Multi/00611/2013) and FEDER-European Regional Development Fund through COMPETE 2020-Operational Programme Competitiveness and Internationalization (project: POCI-01-0145-FEDER-006922). The geomagnetic field data of Colaba Observatory used in this Letter was obtained in Colaba Observatory, and provided by the WDC for Geomagnetism, Kyoto (http://wdc.kugi.kyoto-u.ac.jp/wdc/Sec3.html). B.V., S.M., and Y.E. are supported by Indo-Japan research project funded by Department of Science and Technology, Govt. of India and JSPS, Japan (DST/INT/JSPS/P-137/2012). This study is one of results of the projects HISTIGUC (PTDC/FER-HFC/30666/2017) and MAG-GIC (PTDC/CTA-GEO/31744/2017), the JSPS grant-in-aids 15H05812 (PI: K. Kusano), JP15H05816 (PI: S. Yoden), and JP17J06954 (PI: H. Hayakawa), the Unit of Synergetic Studies for Space of Kyoto University, BroadBand Tower, and the Department of Economy and Infrastructure of the Junta of Extremadura through project IB16127 and grant GR18097 (co-financed by the European Regional Development Fund), and by the Ministerio de Economía y Competitividad of the Spanish Government (CGL2017-87917-P). A.B. was supported by the NASA Van Allen Probes Mission. Y.N. was supported by JSPS Overseas Research Fellowship Program. D.J.K. was partially supported by AFOSR grant No. FA9550-17-1-0258. Some of this material is based upon work supported by the National Center for Atmospheric Research, which is a major facility sponsored by the National Science Foundation under Cooperative Agreement No. 1852977. We gratefully thank Bruno Besser for providing Hungarian records with translations, and Atsuki Shinbori and Masahito Nosé for advice on the evaluation of Sq variation. We also acknowledge the anonymous reviewer for discussions and suggestions that helped to improve our manuscript.

Appendix
Historical Sources of Auroral Observations

Monthly Weather Reports, v. 31, p. 593
Astrophysical Journal, v. 31, pp. 209–213
Nature, v. 69, pp. 9 and 158
Journal of the British Astronomical Association, v. 14, pp. 31–32

Annals of the Observatory of Lucien Libert, v. 11, p. 31
Popular Astronomy, v. 12, p. 288
Ciel et Terre, v. 24 , pp. 420–420
Los Angeles Times 1903 November 1 2
Astronomische Nachrichten, v. 164, pp. 77 and 355
Idõjárás, v. 7, pp. 346–349
Uránia, v. 4, pp. 476–478
Gippsland Times, 1903 November 2, p. 3
The Riverine Herald, 1903 November 2, p. 2
Daily Telegraph, 1903 November 2, p. 2
Traralgon Record, 1903 November 3, p. 2
The Horsham Times, 1903 November 3, p. 2
Camden News, 1903 November 5, p. 4
The Broadford Courier and Reedy Creek Times, 1903 November 6, p. 2
The North Eastern Ensign, 1903 November 6, p. 2
The Walcha Witness and Vernon County Record, 1903 November 7, p. 2
The Grenfell Record and Lachlan District Advertiser, 1903 November 7, p. 2
Cromwell Argus, 1903 November 3, p. 1
Marlborough Express, 1903 November 3, p. 1
Herald Democrat, 1903 November 1, p. 2
The Chicago Sunday Tribune, 1903 November 1, p. 8

ORCID iDs

Hisashi Hayakawa https://orcid.org/0000-0001-5370-3365
Paulo Ribeiro https://orcid.org/0000-0002-4430-7149
José M. Vaquero https://orcid.org/0000-0002-8754-1509
María Cruz Gallego https://orcid.org/0000-0002-8591-0382
Ankush Bhaskar https://orcid.org/0000-0003-4281-1744
Denny M. Oliveira https://orcid.org/0000-0003-2078-7229
Yuta Notsu https://orcid.org/0000-0002-0412-0849
Víctor M. S. Carrasco https://orcid.org/0000-0001-9358-1219
Yusuke Ebihara https://orcid.org/0000-0002-2293-1557

References

Allen, J., Frank, L., Sauer, H., & Reiff, P. 1989, EOS, 70, 1479
Araki, T. 2014, EP&S, 66, 164
Baker, D. N., Balstad, R., Bodeau, J. M., et al. 2008, Severe Space Weather Events-Understanding Societal and Economic Impacts: A Workshop Report (Washington, DC: The National Academies Press)
Bauer, L. A. 1904, TeMAE, 9, 25
Beer, J., Blinov, A., Bonani, G., et al. 1990, Natur, 347, 164
Berggren, A.-M., Beer, J., Possnert, G., et al. 2009, GeoRL, 36, L11801
Boteler, D. H. 2019, SpWea, 17, 1427
Clette, F., & Lefévre, L. 2016, SoPh, 291, 2629
Cliver, E. W., & Dietrich, W. F. 2013, JSWSC, 3, A31
Daglis, I. A., Thorne, R. M., Baumjohann, W., & Orsini, S. 1999, RvGeo, 37, 407
Fowler, A. 1903, Natur, 69, 6
Garcia, H. A., & Dryer, M. 1987, SoPh, 109, 119
Gonzalez, W. D., Joselyn, J. A., Kamide, Y., et al. 1994, JGR, 99, 5771
Gopalswamy, N., Barbieri, L., Cliver, E. W., et al. 2005, JGRA, 110, A09S00
Gopalswamy, N., Xie, H., Yashiro, S., et al. 2012, SSRv, 171, 23
Hayakawa, H., Ebihara, Y., Cliver, E. W., et al. 2019a, MNRAS, 484, 4083
Hayakawa, H., Ebihara, Y., Willis, D. M., et al. 2018, ApJ, 862, 15
Hayakawa, H., Ebihara, Y., Willis, D. M., et al. 2019b, SpWea, 17, 1553
Ichimoto, K., & Kurokawa, H. 1984, SoPh, 93, 105
Jones, H. S. 1955, Sunspot and Geomagnetic-Storm Data derived from Greenwich Observations, 1874-1954 (London: HMSO)
Kilpua, E. K. J., Olspert, N., Grigorievskiy, A., et al. 2015, ApJ, 806, 272
Klotz, O. J. 1904, TeMAE, 9, 188
Knipp, D. J., Ramsay, A. C., Beard, E. D., et al. 2016, SpWea, 14, 614
Lefévre, L., Vennerstrøm, Su., Dumbović, M., et al. 2016, SoPh, 291, 1483
Lockwood, M., Finch, I. D., Chambodut, A., et al. 2018, JSWSC, 8, A58
Lockyer, W. J. S. 1903, Natur, 67, 9
Love, J. J., Hayakawa, H., & Cliver, E. W. 2019a, SpWea, 17, 37
Love, J. J., Hayakawa, H., & Cliver, E. W. 2019b, SpWea, 17, 1281
Marchant, J. W. A. 1904, Department of Lands and Survey (Christchurch: Houses of the General Assembly), 1904
Maunder, E. W. 1903, Knowledge, 26, 275
McCracken, K. G., & Beer, J. 2015, SoPh, 290, 3051
Mekhaldi, F. 2019, Cosmogenic radionuclides in environmental archives A paleo-perspective on space climate and a synchronizing tool for climate records, Doctoral thesis, Univ. Lund
Meng, X., Tsurutani, B. T., & Mannucci, A. J. 2019, JGRA, 124, 3926
Moos, N. A. F. 1910, Magnetic Observations made at the Government Observatory Bombay, for the Period 1846 to 1905 and their Discussions, Part 1, Magnetic Data and Instruments, Bombay, the Government Central Press
Okada, T. 1904, TeMAE, 9, 33
OPCN 1906, Annales de l'observatoire physique central Nicolas Supplement, Irkoutsk
Ribeiro, P., Vaquero, J. M., Gallego, M. C., & Trigo, R. M. 2016, SpWea, 14, 464
Riley, P., Baker, D., Liu, Y. D., et al. 2018, SSRv, 214, 21
Royal Observatory 1905, Greenwich Photo-heliographic Results 1903 (Edinburgh: HM Stationery Office)
Sugiura, M. 1964, Hourly values of equatorial Dst for the IGY, Ann. Int. Geophys. Year, 35 (Oxford: Pergamon), 9
Thébault, E., Finlay, C. C., Beggan, C. D., et al. 2015, EP&S, 67, 79
Tsurutani, B. T., Gonzales, W. D., Lakhna, G. S., & Alex, S. 1903, JGR, 108, A7
Usoskin, I. G., & Kovaltsov, G. A. 2012, ApJ, 757, 92
WDC for Geomagnetism, Kyoto, Nose, M., Iyemori, T., Sugiura, M., & Kamei, T. 2015, Geomagnetic Dst Index
Zi-Ka-Wei 1906, Observatoire magnétique et météorologique, Chang-hai impremerie de la mission catholique, Vol. 29